ChemR23 induces smooth muscle cell phenotypic switching to stimulate vascular calcification

Miguel Carracedo[1], Gonzalo Artiach[1], Anna Witasp[2], Joan Clària[3], Mattias Carlström[4], Andres Laguna-Fernandez[1], Peter Stenvinkel[2], Magnus Bäck[1,5]

[1]Department of Medicine Solna Karolinska Institutet. [2]Division of Renal Medicine, Department of Clinical Science, Intervention and Technology, Karolinska Institutet, Campus Flemingsberg, Stockholm, Sweden. [3]Department of Biochemistry and Molecular Genetics, Hospital Clínic-IDIBAPS and Department of Biomedical Sciences, University of Barcelona, Barcelona, Spain. [4]Department of Physiology and Pharmacology, Karolinska Institutet, Stockholm, Sweden. [5]Theme Heart and Vessels, Divison of Valvular and Coronary Disease, Karolinska University Hospital, Stockholm, Sweden.

Author for correspondence: Magnus Bäck

Department of Cardiology
S1:02
Karolinska University Hospital
17176 Stockholm
Sweden

Abstract

Rationale: Medial artery calcification is a common feature in chronic kidney disease (CKD) and diabetes mellitus. The de-differentiation of vascular smooth muscle cells (VSMC), an increased extracellular matrix production, downregulation calcification inhibitors, and phenotypic transition of VSMCs into osteoblast-like cells contribute to medial calcification. The G-protein coupled receptor ChemR23 is upregulated during bone development, and plays a role in osteoblastic differentiation of stem cells. ChemR23 is highly expressed in VSMCs, however its role in VSMC biology and vascular calcification is unknown.

Objective: The aim of the present study was to establish the role of ChemR23 in VSMCs fate and vascular calcification.

Methods and Results: In the present study, VSMC ChemR23 protein expression was identified in uremic arteries in which a multivariate analysis revealed that ChemR23 mRNA levels were independently associated with collagen type 1 (Col1A1) gene expression. In support of a causality for this association, genetic deletion of ChemR23 in mice prevented VSMC de-differentiation, maintaining a contractile phenotype characterized by low Col1A1 production, high expression of Calponin (CNN1) and alpha smooth muscle actin (ACTA2), and low proliferation. Moreover, ChemR23 deficient mice exhibited increased anti-calcifying signaling and a reduction in osteogenic differentiation characterized by higher osteoprotegerin (OPG) levels and lower Runt-related transcription factor 2 (RUNX2) expression, respectively, thus preventing phosphate induced vascular calcification both *in vitro* and *in vivo*. Finally we show that stimulation of ChemR23 with its ligand, RvE1, partially reduces calcification without altering the VSMC phenotype.

Conclusions: Taken together, this data demonstrate a novel role of ChemR23 in VSMC phenotype switching, which favors osteoblastic differentiation and vascular calcification.

Introduction

Medial artery calcification is a pathophysiological process characterized by the deposition of calcium and phosphate, principally in the form of hydroxyapatite, surrounding vascular smooth muscle cells (VSMCs) and within the elastic laminae layers of arteries. Originally, cardiovascular calcification was considered as a passive degenerative process associated with age, but it is now recognized as an active process involving pro-inflammatory cues, and phenotypical changes of cells. Medial calcification is highly prevalent in disorders characterized with premature vascular ageing, such as chronic kidney disease (CKD), and diabetes mellitus, and contributes to increased cardiovascular morbidity and mortality.[1-4]

Under physiological conditions VSMCs are responsible of maintaining a variable contractile tone of the arteries. To achieve this, they express a wide variety of contractile proteins such as alpha smooth muscle actin (ACTA2), and Calponin (CNN1). In response to injury VSMCs undergo phenotypical switching and de-differentiation characterized by a modified proliferation, contractility and increased extracellular matrix production.[5] Under hyperphosphatemia and hypercalcemia, typically present in the uremic milieu, the physicochemical deposition of hydroxyapatite crystals in the arteries is prevented by calcification inhibitors, such as matrix-gla protein (MGP), fetuin-A, and osteoprotegerin (OPG) present in the circulation and locally produced by VSMCs. However, the downregulation of these inhibitors, the direct effects of phosphate and calcium, and the upregulation of pro-calcifying pathways such as the Runt-related transcription factor 2 (RUNX2) and bone morphogenic protein 2 (BMP-2), lead to the phenotypical transformation of VSMCs into osteoblast-like cells and cell death, necessary for medial calcification.[6] Nonetheless, the molecular pathways leading to this phenotypic switch are not fully understood.

ChemR23 is a G-protein coupled receptor, which is upregulated during bone development. Moreover, studies in mesenchymal stem cells have implicated a role for ChemR23 signaling in in osteoblast differentiation.[7, 8] However, apart from being highly expressed in VSMCs,[9] the role of ChemR23 in VSMC osteogenic differentiation has remained hitherto unexplored. Nevertheless, some indications for a role of ChemR23 in vascular calcifications have emerged from studies of the two known ChemR23 ligands, *i.e.* the omega-3-derived lipid mediator, resolvin E1 (RvE1) [10, 11] and the adipokine chemerin. Indeed, the RvE1 precursor eicosapentaenoic acid (EPA) prevents vascular calcification in different animal models although the mechanism involved remains to be established [12, 13]. In contrast, circulating chemerin has been associated with diabetes mellitus, cardiovascular disease, obesity and CKD.[14] Nevertheless, in incident dialysis patients, elevated chemerin is associated with a survival advantage, despite associations with increased inflammation and dyslipidemia.[15]

Based on the above, the aim of the present study was to establish the role of ChemR23 in VSMCs fate and vascular calcification.

Material and Methods

Patient population and TaqMan low density array

Adult patients undergoing living donor kidney transplantation (RTx) at the Dept. of Transplantation Surgery at the Karolinska University Hospital were invited to participate in the study. All participants provided written informed consent and the Regional Ethical Review Board in Stockholm approved the study. Basic patient characteristics are outlined in Table 1. The most common causes of CKD were chronic glomerulonephritis (n=27), polycystic kidney disease (n=10), interstitial nephritis (n=3) and other (or unknown) causes (n=21). The median systolic and diastolic blood pressures were 142 (IQR 129-152) and 86 (IQR 74-93) mmHg, respectively. The most commonly used medications were erythropoietin-stimulating agents (84%), non-calcium-based phosphate binders (75%), calcium-based phosphate binders (4%) and loop-diuretics (62%). Commonly used anti-hypertensive treatments were β-blocking agents (52%) and ACE-i/ARBs (72%); 30% of the patients were on statins. One patient was on warfarin. In this group of younger patients only five had clinical signs of cerebrovascular, cardiovascular, and/or peripheral vascular disease (grouped as CVD). Three had clinical signs of ischemic heart disease and two had peripheral ischemic atherosclerotic vascular disease.

Isolation of RNA from epigastric artery and subsequent cDNA preparation were executed as described before.[3] Gene expression was analyzed using a TaqMan Low Density Array on a QuantStudioTM 7 Flex Real-Time PCR system (LifeTechnologies, Carlsbad, CA, USA) according to standard protocol. Amplification profiles for each sample and target were normalized against endogenous control genes (mitochondrially encoded 16S RNA, MT-RNR2; TATA box binding protein, TBP; and glyceraldehyde-3-phosphate dehydrogenase, GAPDH). Ct above 35, bad passive reference signal, noise spikes and high noise were removed from further analyses. The data were analyzed using ExpressionSuite®Software v1.0.4 (Applied Biosystems, Life Technologies, Carlsbad, CA, USA).

SMC isolation and culture

Mouse aortic VSMCs were isolated from 8-12 week old male mice according to previously published protocols[16, 17]. In brief, aortic arches from 3 mice were isolated, fat and adventitia removed, and digested in a sterile mixture of 1mg/mL collagenase type II (Worthington) and 0.3mg/mL elastase (Sigma, E0127) in DMEM with 10% FBS for 90 minutes at 37˚C and 5% CO_2. Cell suspension was spun down, resuspended in cell culture medium (DMEM, 10% fetal calf serum, 100 units/ml penicillin, 100 µg/ml streptomycin, 1mM sodium pyruvate, 10 mM HEPES and 2 mM L-glutamine) and plated. Cells were passaged using trypsin when they reached 80% confluency.

Cell stimulation

All experiments were performed in between passage 3 and 5 with an initial cell density of 10,000 cells/cm^2 and cultured in cell culture medium with 5% FBS. *In vitro* calcification was induced by culturing VSMCs for 9 days in cell culture media supplemented with 2.6mM inorganic phosphate (Sigma), prepared as described previously.[13] Cells were stimulated with 20 ng/mL of recombinant mouse BMP-2 (R&D) for 30 minutes washed with ice-cold PBS and protein was immediately extracted. Cells were stimulated with 100nM RvE1 (Cayman) or vehicle (0.01% ethanol).

Experimental animals

ChemR23 deficient mice on a C57BL/6 background were purchased from Deltagen. In-house bred C57BL/6 were used as wild-type controls. Fat-1 transgenic mice, which encode the n-3 fatty acid desaturase, thus producing n-3 fatty acids from n-6 type[18], were bred as previously described[19]. Specific primers for ChemR23, and Fat1 were used to genotype the experimental animals (Supplementary Table 1). All animal experiments were conducted in accordance with guidelines from the Directive 2010/63/EU of the European Parliament on the protection of animals used for scientific purposes and were approved by the Ethical Committee of Northern Stockholm.

Mice were fed a cholesterol-free standard chow diet (R70, Lantmännen). At 20 weeks of age, mice were fed an omega-6 rich diet (10% v/w) for 2 weeks, before first cholecalciferol injection (prepared as described bellow), diet was continued until euthanasia.

Vascular calcification was induced by injecting mice subcutaneously with 500 IU/g a day of Vitamin D_3 (cholecalciferol) for three days and euthanized seven days after last injection. A stock solution of 132,000 IU/mL was prepared by dissolving 66 mg cholecalciferol in 200 µL of ethanol + 1.4 mL cremophor +18.4 mL H2O (with 750 mg dextrose), all from Sigma. Stock solution was prepared fresh the first day of injections and stored in the dark at 4 ˚C.

Animals were euthanized by CO_2 asphyxiation. Blood was collected by cardiac puncture into Heparin-coated tubes and vascular perfusion was performed with 10 ml sterile RNase-free phosphate-buffered saline (PBS). Blood counts were analyzed using an automated hematology analyzer (Scil Vet abc hemocounter).

Aortic root sectioning and calcification quantification

Aortic roots were embedded in OCT and serially sectioned from the proximal 1 mm of the aortic root on a cryostat. Alizarin Red stained sections were used to evaluate total calcification, which was determined by measuring 5 sections collected at every 100 µm over the 200-600 µm segment of the aortic root. For each section, images were captured with a Nanozoomer slide scanner (Hamamatsu), analyzed, and the surface areas of the calcification(s) and of the entire vessel were measured with the NDP.view2 software (Hamamatsu).

Calcium quantification

Total calcium was determined by the chromogenic complex formed between calcium ions and *o*-cresolphthalein. In brief, right carotid was isolated, dried, incubated in 0.6M HCl overnight at 37 ˚C, and dilutions of the supernatant measured according to manufacturer's protocol (Sigma).

Bone mineral density measurement

Femurs were isolated, cleaned from muscle and connective tissue, placed in 4% formaldehyde for 48h and stored in 70% ethanol. Bone mineral density was measured *ex vivo* using dual-energy x-ray absorptiometry densitometry (Lunar PIXImus, GE healthcare).

Plasma and supernatant measurements

Plasma phosphate and pyrophosphate were measured according to manufacturer's protocol (Abcam). Plasma OPG concentration was measured by ELISA (R&D). Cell supernatants were assayed with the same kits after centrifugation at 400g for 5min.

Alizarin red staining

2% alizarin red was diluted in dH_2O, filtered, and pH adjusted to 4.1-4.3 with either 10% ammonium hydroxide or HCl. For histochemistry, formaldehyde fixed slides were hydrated, incubated for 2 minutes in 2% Alizarin Red, dehydrated in acetone, followed by acetone-xylene (1/1 v/v) solution, and cleared in xylene. Slides were mounted with a synthetic mounting medium (PERTEX, Histolab). Alizarin red staining extraction and quantification of *in vitro* cultured cells was performed according to previously published protocol using an acetic acid based extraction method. [15]

Cell proliferation

Measurement of cellular proliferation was determined by estimating ^{3}H-Thymidine incorporation into DNA. Quiescent VSMC were cultured for 72h. 1 µCi of ^{3}H-Thymidine (Amersham) was added 12h before the end of the experiment. Cells were harvested on glass fiber filters and ^{3}H-Thymidine activity (counts per minute) was measured in a liquid scintillation counter (Wallac, 1450 Microbeta Plus).

RNA extraction and quality assessment

Total RNA from tissue and cells in culture was isolated using the RNeasy Lipid Tissue Mini kit (Qiagen). RNA concentrations were quantitated spectrophotometrically at 260 nm (Thermo Scientific), and quality was evaluated on a 2100 Bioanalyzer (Agilent) using RNA 6000 NANO chips to assess the RNA integrity number.

TaqMan Real-Time PCR

Reverse-transcription was performed using High Capacity RNA-to-cDNA Kit (Applied Biosystems). Quantitative real-time PCR reaction was developed on a 7900HT Fast Real-Time PCR system (Life Technologies) using Taqman Assay-on-Demand from Life Technologies (Supplementary Table 2). The relative mRNA expression of the target genes was quantified by the $2^{-\Delta CT}$ or $2^{-\Delta\Delta CT}$ method using TATA binding protein (TBP) as endogenous control.

Immunoblotting

Protein extracts were prepared by lysing the cells with RIPA buffer (Sigma) containing a protease and phosphatase inhibitor cocktail (Roche). Protein concentrations were determined using DC-Protein Assay (BioRad) following manufacturer's protocol. 15 µg of the protein extracts were diluted (1:1) in Laemmli sample buffer (BioRad) containing 2.5% β-mercaptoethanol (Sigma) (immunoblots against Col1A1 were β-mercaptoethanol free). Diluted samples were incubated 5 min at 95° C, loaded on a MiniProtean TGX 4-12% gel (BioRad), and finally transferred to a PVDF membrane (BioRad). The membranes were blocked using non-fat dry milk and incubated with primary antibodies against Col1A1 (Merck), p-SMAD 1/5/8 (Cell signaling) and the loading control vinculin (Abcam) overnight at 4 ˚C. Membranes were then washed and incubated in fluorescently labelled antibodies (Li-cor) for 1 hour at room temperature, and signal was detected using Odyssey CLx imagin system (Li-cor).

Immunofluorescence

Cells were seeded in crystal chamber slides (Falcon). After stimulation, cells were washed twice in PBS and fixed in 4% formaldehyde. The staining was performed according to the antibody manufacturer´s protocol. In brief, cells were washed three times in wash buffer (TBS + 0.1% tween). Cells were then permeabilized with ice-cold methanol and washed. Blocking was performed in 5% normal horse serum diluted in wash buffer. Primary antibody was incubated over-night at 4 ˚C. Secondary antibody was incubated for 1 hour at room temperature.

Statistical analyses

Results are expressed as mean ± S.D. or median with 95% CI. Statistical significance of differences for normally-distributed data was assessed with Student *t* test when comparing two groups, and with one-way or two-way ANOVA as appropriate followed by recommended post hoc tests, for multiple comparisons. Statistical significance was assigned at $p<0.05$. Statistical analysis were performed using GraphPad Prism 7 (GraphPad Software Inc, CA, USA).

Results

Collagen is related with ChemR23 expression in human and murine smooth muscle cells

The baseline characteristic of the CKD patient cohort are shown in Table 1. Stratification according to treatment groups revealed that hemodialysis (HD) patients exhibited significantly higher levels of hsCRP, whereas other clinical parameters did not significantly differ between patients with or without either peritoneal dialysis (PD) or HD (Table 1). Immunofluorescence stainings revealed ChemR23 expression in the media layer of the arterial wall, co-localizing with the smooth muscle cell marker ACTA2 (Fig 1A). The mRNA levels of ChemR23 were subsequently examined together with a panel of different smooth muscle associated proteins with importance for VSMC differentiation and calcification mRNA. Multivariate analysis for the association of ChemR23 mRNA with these other mRNA levels after adjusting for age, sex and diabetes (Table 2) revealed collagen type 1 (Col1A1) as an independent predictor of ChemR23 mRNA. The strong association between ChemR23 mRNA and Col1A1 mRNA levels is depicted in (Fig 1B). Expression analysis of Col1A1 in VSMCs derived from either wild-type (WT) or ChemR23 knock-out (KO) mice revealed significantly lower mRNA and protein levels in KO compared with WT VSMCs (Fig 1C).

ChemR23 deletion alters the smooth muscle cell phenotype

Since our finding in human arteries and murine VSMCs suggested that ChemR23 expression was associated with a sythetic VSMC phenotype, we subsequently performed comparative analysis between WT and KO murine aortic VSMCs. Whereas WT cells exhibited decreased mRNA levels and CNN1 and ACTA2, after 9 days in culture, knock-out (KO) cells retained the expression levels of these VSMC phenotypic markers. As a result, KO cells expressed significantly higher levels of CNN1 and ACTA2 (Fig 2A). KO cells proliferated significantly compared WT cells (Fig 2B). The mRNA levels encoding proteins relevant for calcification are shown in Fig 2D. Whereas BMP2 mRNA levels increased to a similar degree in both wild-type and KO VSMCs after nine days in culture, RUNX2 expression remained unchanged. OPG expression increased significantly overtime only in only KO VSMCs, resulting in significantly higher OPG mRNA levels in KO than in WT VSMCs at nine days in culture (Fig 2D).

ChemR23 deficient VSMCs exhibit reduced calcification and osteogenic signaling

Given the differential expression levels of pro- and anti-calcifying factors in cells derived from WT and ChemR23 KO mice, we next evaluated the differential VSMC calcifying phenotype between WT and KO cells cultured in a high phosphate media. Calcification was significantly higher in WT as compared with KO cells (Fig 3A). No significant differences in pyrophosphate levels were observed between the genotypes (WT: 2.5 ± 0.16 vs KO: 2.9 ±0.15, p=0.08). RUNX2 expression was significantly lower in KO cells (Fig 3B). Although BMP-2 mRNA levels were not significantly different between WT and KO cells (Fig 3B), the response to BMP2 stimulation in terms of SMAD 1/5/8 phosphorylation was significantly lower in KO compared with WT cells (Fig 3C). Finally, in line with results obtained during culture in normal media, KO cells exhibited higher mRNA levels of OPG under high phosphate conditions. Concomitantly, higher OPG protein levels were observed in the supernatants of KO VSMCs (Figure 3D).

The ChemR23 ligand RvE1 decreases calcification and osteogenic signaling without altering VSMC phenotype.

Nine days of culture in high phosphate media containing RvE1 (100 nM) significantly reduced calcification in WT, but not in KO VSMCs as compared with vehicle treated cells (Fig 4A). Gene expression analysis revealed a significant difference in the fold changes between WT and KO cells in BMP2 mRNA levels. Moreover RvE1 significantly reduced BMP2 mRNA levels in WT cells 95% CI [0.4028, 0.909], while showing no significant effect in KO cells 95% CIs [-0.211, 2.935] (Fig 4B). No significant alterations of RUNX2 and OPG mRNA were observed in either wild-type or KO (Fig 4B).

Likewise, CNN1, ACTA2 and Col1A1 mRNA levels remained unchanged upon RvE1 treatment both in WT and KO cells (Fig 4C).

ChemR23 deletion, but not Fat1 transgene, protects from VitD3 induced vascular calcification in vivo:

Based in the *in vitro* results presented above ChemR23 KO cells showed reduced calcification, and the omega-3-derived lipid mediator RvE1 inhibited calcification in WT cells, vascular calcification was induced *in vivo* by means of Vitamin D_3 injections into WT, ChemR23 KO, and Fat-1 transgenic mice. As shown in Fig 5A, ChemR23 KO mice exhibited significantly reduced calcification in the aortic root compared with WT mice, whereas the calcification observed in Fat-1 transgenic mice was not significantly different from controls (Fig 4A-B). In line with these results, analysis of the Ca^{+2} content in the right carotid revealed significantly lower levels in KO compared with WT mice (Figure 5C). Plasma phosphate levels were significantly higher in KO than in WT mice (Figure 5D), bone mineral density was significantly lower in KO mice compared with WT mice (Figure 5E). Plasma OPG was significantly higher in KO mice compared with WT mice (Figure 5F). Gene expression analyses performed in thoracic aortas revealed a significant increase in OPG mRNA in KO mice and a significant decrease in RUNX2 mRNA in KO mice when compared with WT mice (Figure 5G). At the same time, the VSMC markers CNN1 and ACTA2 were significantly increased in KO mice, and Col1A1 gene expression was significantly lower in KO mice compared with WT mice (Figure 5H).

Discussion

Three major observations in the present study support a novel role for ChemR23 in VSMC biology and vascular calcification. First, we detected arterial VSMC ChemR23 expression and identified Col1A1 as an independent predictor of arterial ChemR23 mRNA levels in CKD patients. Second, genetic deletion of ChemR23 in mice reduced Col1A1 and inherently protected VSMCs against a phenotypic de-differentiation and osteoblastic transformation, which translated into reduced vascular calcification both *in vitro* and *in vivo*. Third, the calcification susceptibility in ChemR23-expressing VSMCs was reversed by the ChemR23 agonist RvE1, without alteration of the VSMC phenotype. Taken together, these results suggest that ChemR23 contributes to a calcifying VSMC phenotype.

Through the exploration of arterial gene expression patterns in patients with CKD, our multivariate analysis identified ChemR23 as an independent predictor of increased Col1A1 expression, hence raising the notion that ChemR23 expression may be associated with VSMC de-differentiation into a synthetic phenotype. Such phenotypic transition, with loss of contractile capacity and the acquisition of less differentiated features with high synthetic and proliferative activity[20] is observed in several vascular pathological conditions[5], and also occur spontaneously *in vitro* in primary VSMCs cultures. In support of a causal link between ChemR23 expression and increased Col1A1, ChemR23 deficient murine VSMCs expressed less Col1A1, indicating a less synthetic phenotype and a resilience to this time-in-culture de-differentiation observed in wild-type VSMCs. Consequently, ChemR23 deficient VSMCs retained contractile markers and exhibited a reduced proliferation compared with wild-type VSMCs. Although not previously assessed in VSMC, the latter observation corroborates results in mesenchymal stem cells, in which ChemR23 knock-down by RNA interference directly impairs the G_2/M phase of the cell cycle through a loss of cyclins A2 and B2[21].

In addition to acquiring a synthetic and proliferative phenotype, increased BMP-2 release is also part of the de-differentiation process in SMC primary cultures [22], which was confirmed in the present study. Intriguingly, ChemR23 KO cells were resistant to BMP-2-induced phosphorylation of SMAD 1/5/8, which is the activator of its pro-calcifying signaling[23, 24]. In line with this finding, we show that ChemR23 KO VSMCs exhibited less calcification compared with WT cells when cultured under pro-calcifying conditions. This was accompanied by less osteogenic differentiation, as measured by phosphate-induced expression of RUNX2, which is the signature transcription factor of an osteoblastic and pro-calcifying VSMC phenotype[25-27].

In a pro-calcifying milieu, VSMCs actively produce anti-calcifying mediators that protect from osteogenic differentiation and vascular calcification[6]. One such example is OPG[28, 29], which was highly increased in KO as compared with WT VSMCs. Since the latter difference was observed both under normal and pro-calcifying conditions, these results suggest an inherent repression of osteoblastic differentiation in ChemR23 deficient cells, which translates into protection from phosphate-induced calcification. The reduced osteogenic differentiation by OPG in VSMCs may be associated with decreased Notch1 signaling[30], and in support of a ChemR23/OPG/Notch1 signaling axis, mesenchymal stem cells derived from KO mice exhibit decreased collagen levels and reduced mineralization compared with WT only after Notch abrogation by γ-secretase inhibitors[8]. These observations suggest that deletion of the ChemR23 receptor induces a sensitivity to Notch1 inhibition which prevents osteoblastic transformation of mesenchymal cells and thus maintaining a contractile VSMC phenotype. In contrast, bone-marrow-derived stem cells exhibit an increased osteoblastic transcriptional signature and increased *in vitro* mineralization after ChemR23 knock-down[31], which would be consistent with Notch1 preventing dedifferentiation of hematopoietic stem cells[32].

There are several agonists for the ChemR23 receptor, which potentially could transduce biological effects in VSMCs. For example, RvE1 reduces human PDGF-induced VSMC proliferation[9], but its effects on VSMC calcification have not previously been explored. Indeed, the reduction in calcification and BMP-2 levels in response to RvE1 in WT, but not in KO cells, support that RvE1 reduced calcification by means of ChemR23. In contrast, characteristic markers of a contractile and/or osteoblast phenotype were not altered by this agonist in either WT or KO VSMCs, indicating that the acquired VSMC phenotype cannot be reversed by RvE1. Although RvE1 has been previously reported to prevent the downregulation of OPG induced by pro-inflammatory conditions in osteoblasts[33] RvE1 did not alter OPG mRNA levels in VSMCs in the present study. Interestingly, the ligand-induced

reduction of VSMC calcification and BMP-2 levels, without altering the VSMC phenotype or OPG levels, argue in favor of differential mechanisms as compared with the inherent VSMC phenotypic changes associated with reduced calcification in ChemR23-deficient cells. In fact, a dual role for ChemR23 in VSMC calcification emerges, in which the absence of ChemR23 confer a phenotypic protection against calcification whereas the calcification susceptibility exhibited by ChemR23-expressing SMCs can be rescued by receptor agonists through alternative pathways.

Vitamin D_3 treatment in mice induces vascular calcification under conditions that closely resemble the calcifying conditions used in the *in vitro* studies, e.g. high phosphate without inflammatory stimuli. Indeed, KO mice exhibited significantly less vitamin D_3-induced vascular calcification in the aortic root and carotid artery as compared with WT animals, despite more pronounced hyperphosphatemia. These observations were accompanied by a lower bone mineral density in KO mice, consistent with the role of ChemR23 in bone development and osteoclastogenesis, potentially making KO mice more susceptible to high dose vitamin D_3-induced bone resorption[33-35]. Importantly, the aortic transcriptional profile in KO mice was consistent with a preserved contractile, non-synthetic and non-osteoblastic SMC phenotype. In addition, KO mice exhibited increased aortic and circulating levels of OPG, further reinforcing the importance of this vascular calcification inhibitor in the protection conferred by ChemR23 deficiency in the present study. The causal involvement of both RUNX2 and OPG as a driver and inhibitor, respectively, of vitamin D_3-induced vascular calcification has been demonstrated in previous *in vivo* studies[25, 36, 37]. Moreover, similar to our *in vitro* findings, we found a reduced Col1A1 expression in KO mice, which may contribute to a further inhibition of calcium deposits in the vascular wall [38].

To assess the role of agonist-induced ChemR23 signaling, we also assessed vitamin D_3-induced vascular calcification in Fat1 transgenic mice, which have been reported to have an increased formation of the ChemR23 ligand RvE1[39]. However, the latter mice did not exhibit any significant change in vascular calcification compared with non-transgenic mice. Although previous reports on Omega-3 fatty acids have indicated reduced calcification[12, 13], there are several reasons for the lack of beneficial effects of the Fat1 transgene in VSMC calcification. First, RvE1 did not alter VSMC phenotype *in vitro*, and the lack of effect of the Fat-1 transgene underlines the importance of the VSMC phenotypic preservation in ChemR23-deficient SMCs. Second, *in vitro,* RvE1 reduced BMP2, which is a vitamin D receptor activator-induced gene which expression levels appeared irreversible *in vitro* in the present study. Third, it should be acknowledged that although the RvE1 precursor EPA was increased, RvE1 was not measured in this study and it cannot be excluded that the lack of inflammatory stimuli in the model used may not stimulate RvE1 formation from EPA.

In summary, the present study identifies ChemR23 as an independent predictor of vascular Col1A1 in human vessels and provides evidence that ChemR23 deletion in mice confers protection against VSMC dedifferentiation and vascular calcification both *in vitro* and *in vivo*, characterized by reduced osteogenic differentiation and increased anti-calcification signaling. Furthermore, the ChemR23 agonist RvE1 could partly reverse the *in vitro* calcification without altering VSMC phenotype. In conclusion, ChemR23 is a regulator of VSMC phenotype switching, which favors osteoblastic differentiation and therefore vascular calcification.

References

1. Iribarren C, Sidney S, Sternfeld B and Browner WS. Calcification of the aortic arch: risk factors and association with coronary heart disease, stroke, and peripheral vascular disease. *Jama*. 2000;283:2810-5.
2. Blacher J, Guerin AP, Pannier B, Marchais SJ and London GM. Arterial calcifications, arterial stiffness, and cardiovascular risk in end-stage renal disease. *Hypertension*. 2001;38:938-42.
3. Stenvinkel P, Luttropp K, McGuinness D, Witasp A, Qureshi AR, Wernerson A, Nordfors L, Schalling M, Ripsweden J, Wennberg L, Soderberg M, Barany P, Olauson H and Shiels PG. CDKN2A/p16INK4(a) expression is associated with vascular progeria in chronic kidney disease. *Aging (Albany NY)*. 2017;9:494-507.
4. Stabley JN and Towler DA. Arterial Calcification in Diabetes Mellitus: Preclinical Models and Translational Implications. *Arterioscler Thromb Vasc Biol*. 2017;37:205-217.
5. Lacolley P, Regnault V, Nicoletti A, Li Z and Michel JB. The vascular smooth muscle cell in arterial pathology: a cell that can take on multiple roles. *Cardiovasc Res*. 2012;95:194-204.
6. Leopold JA. Vascular calcification: Mechanisms of vascular smooth muscle cell calcification. *Trends Cardiovasc Med*. 2015;25:267-74.
7. Methner A, Hermey G, Schinke B and Hermans-Borgmeyer I. A novel G protein-coupled receptor with homology to neuropeptide and chemoattractant receptors expressed during bone development. *Biochem Biophys Res Commun*. 1997;233:336-42.
8. Muruganandan S, Govindarajan R, McMullen NM and Sinal CJ. Chemokine-Like Receptor 1 Is a Novel Wnt Target Gene that Regulates Mesenchymal Stem Cell Differentiation. *Stem Cells*. 2017;35:711-724.
9. Ho KJ, Spite M, Owens CD, Lancero H, Kroemer AH, Pande R, Creager MA, Serhan CN and Conte MS. Aspirin-triggered lipoxin and resolvin E1 modulate vascular smooth muscle phenotype and correlate with peripheral atherosclerosis. *Am J Pathol*. 2010;177:2116-23.
10. Arita M, Bianchini F, Aliberti J, Sher A, Chiang N, Hong S, Yang R, Petasis NA and Serhan CN. Stereochemical assignment, antiinflammatory properties, and receptor for the omega-3 lipid mediator resolvin E1. *J Exp Med*. 2005;201:713-22.
11. Bäck M, Powell WS, Dahlen SE, Drazen JM, Evans JF, Serhan CN, Shimizu T, Yokomizo T and Rovati GE. Update on leukotriene, lipoxin and oxoeicosanoid receptors: IUPHAR Review 7. *Br J Pharmacol*. 2014;171:3551-74.
12. Kanai S, Uto K, Honda K, Hagiwara N and Oda H. Eicosapentaenoic acid reduces warfarin-induced arterial calcification in rats. *Atherosclerosis*. 2011;215:43-51.
13. Nakamura K, Miura D, Saito Y, Yunoki K, Koyama Y, Satoh M, Kondo M, Osawa K, Hatipoglu OF, Miyoshi T, Yoshida M, Morita H and Ito H. Eicosapentaenoic acid prevents arterial calcification in klotho mutant mice. *PLoS One*. 2017;12:e0181009.
14. Ferland DJ and Watts SW. Chemerin: A comprehensive review elucidating the need for cardiovascular research. *Pharmacol Res*. 2015;99:351-61.
15. Yamamoto T, Qureshi AR, Anderstam B, Heimbürger O, Bárány P, Lindholm B, Stenvinkel P and Axelsson J. Clinical importance of an elevated circulating chemerin level in incident dialysis patients. *Nephrol Dial Transplant*. 2010;25:4017-23.
16. Petri MH, Laguna-Fernandez A, Gonzalez-Diez M, Paulsson-Berne G, Hansson GK and Bäck M. The role of the FPR2/ALX receptor in atherosclerosis development and plaque stability. *Cardiovasc Res*. 2015;105:65-74.
17. Petri MH, Laguna-Fernandez A, Tseng CN, Hedin U, Perretti M and Bäck M. Aspirin-triggered 15-epi-lipoxin A(4) signals through FPR2/ALX in vascular smooth muscle cells and protects against intimal hyperplasia after carotid ligation. *Int J Cardiol*. 2015;179:370-2.
18. Kang JX. Fat-1 transgenic mice: a new model for omega-3 research. *Prostaglandins Leukot Essent Fatty Acids*. 2007;77:263-7.
19. Lopez-Vicario C, Alcaraz-Quiles J, Garcia-Alonso V, Rius B, Hwang SH, Titos E, Lopategi A, Hammock BD, Arroyo V and Claria J. Inhibition of soluble epoxide hydrolase modulates inflammation and autophagy in obese adipose tissue and liver: role for omega-3 epoxides. *Proc Natl Acad Sci U S A*. 2015;112:536-41.

20. Rzucidlo EM, Martin KA and Powell RJ. Regulation of vascular smooth muscle cell differentiation. *J Vasc Surg*. 2007;45 Suppl A:A25-32.
21. Muruganandan S, Parlee SD, Rourke JL, Ernst MC, Goralski KB and Sinal CJ. Chemerin, a novel peroxisome proliferator-activated receptor gamma (PPARgamma) target gene that promotes mesenchymal stem cell adipogenesis. *J Biol Chem*. 2011;286:23982-95.
22. Chen NX, Duan D, O'Neill KD and Moe SM. High glucose increases the expression of Cbfa1 and BMP-2 and enhances the calcification of vascular smooth muscle cells. *Nephrol Dial Transplant*. 2006;21:3435-42.
23. Shimizu T, Tanaka T, Iso T, Matsui H, Ooyama Y, Kawai-Kowase K, Arai M and Kurabayashi M. Notch signaling pathway enhances bone morphogenetic protein 2 (BMP2) responsiveness of Msx2 gene to induce osteogenic differentiation and mineralization of vascular smooth muscle cells. *J Biol Chem*. 2011;286:19138-48.
24. Derwall M, Malhotra R, Lai CS, Beppu Y, Aikawa E, Seehra JS, Zapol WM, Bloch KD and Yu PB. Inhibition of bone morphogenetic protein signaling reduces vascular calcification and atherosclerosis. *Arterioscler Thromb Vasc Biol*. 2012;32:613-22.
25. Lin ME, Chen T, Leaf EM, Speer MY and Giachelli CM. Runx2 Expression in Smooth Muscle Cells Is Required for Arterial Medial Calcification in Mice. *Am J Pathol*. 2015;185:1958-69.
26. Lin ME, Chen TM, Wallingford MC, Nguyen NB, Yamada S, Sawangmake C, Zhang J, Speer MY and Giachelli CM. Runx2 Deletion in Smooth muscle Cells Inhibits Vascular Osteochondrogenesis and Calcification but not Atherosclerotic Lesion Formation. *Cardiovasc Res*. 2016.
27. Sun Y, Byon CH, Yuan K, Chen J, Mao X, Heath JM, Javed A, Zhang K, Anderson PG and Chen Y. Smooth muscle cell-specific runx2 deficiency inhibits vascular calcification. *Circ Res*. 2012;111:543-52.
28. Bucay N, Sarosi I, Dunstan CR, Morony S, Tarpley J, Capparelli C, Scully S, Tan HL, Xu W, Lacey DL, Boyle WJ and Simonet WS. osteoprotegerin-deficient mice develop early onset osteoporosis and arterial calcification. *Genes Dev*. 1998;12:1260-8.
29. Callegari A, Coons ML, Ricks JL, Rosenfeld ME and Scatena M. Increased calcification in osteoprotegerin-deficient smooth muscle cells: Dependence on receptor activator of NF-kappaB ligand and interleukin 6. *J Vasc Res*. 2014;51:118-31.
30. Zhou S, Fang X, Xin H, Li W, Qiu H and Guan S. Osteoprotegerin inhibits calcification of vascular smooth muscle cell via down regulation of the Notch1-RBP-Jkappa/Msx2 signaling pathway. *PLoS One*. 2013;8:e68987.
31. Muruganandan S, Roman AA and Sinal CJ. Role of chemerin/CMKLR1 signaling in adipogenesis and osteoblastogenesis of bone marrow stem cells. *J Bone Miner Res*. 2010;25:222-34.
32. Weber JM and Calvi LM. Notch signaling and the bone marrow hematopoietic stem cell niche. *Bone*. 2010;46:281-5.
33. Gao L, Faibish D, Fredman G, Herrera BS, Chiang N, Serhan CN, Van Dyke TE and Gyurko R. Resolvin E1 and chemokine-like receptor 1 mediate bone preservation. *J Immunol*. 2013;190:689-94.
34. Ohira T, Spear D, Azimi N, Andreeva V and Yelick PC. Chemerin-ChemR23 signaling in tooth development. *J Dent Res*. 2012;91:1147-53.
35. Suda T, Takahashi F and Takahashi N. Bone effects of vitamin D - Discrepancies between in vivo and in vitro studies. *Arch Biochem Biophys*. 2012;523:22-9.
36. Price PA, June HH, Buckley JR and Williamson MK. Osteoprotegerin inhibits artery calcification induced by warfarin and by vitamin D. *Arterioscler Thromb Vasc Biol*. 2001;21:1610-6.
37. Morony S, Tintut Y, Zhang Z, Cattley RC, Van G, Dwyer D, Stolina M, Kostenuik PJ and Demer LL. Osteoprotegerin inhibits vascular calcification without affecting atherosclerosis in ldlr(-/-) mice. *Circulation*. 2008;117:411-20.
38. Krohn JB, Hutcheson JD, Martinez-Martinez E, Irvin WS, Bouten CV, Bertazzo S, Bendeck MP and Aikawa E. Discoidin Domain Receptor-1 Regulates Calcific Extracellular Vesicle Release in Vascular Smooth Muscle Cell Fibrocalcific Response via Transforming Growth Factor-beta Signaling. *Arterioscler Thromb Vasc Biol*. 2016;36:525-33.

39. Bilal S, Haworth O, Wu L, Weylandt KH, Levy BD and Kang JX. Fat-1 transgenic mice with elevated omega-3 fatty acids are protected from allergic airway responses. *Biochim Biophys Acta*. 2011;1812:1164-9.

	ALL	CKD 5	PD	HD	*P*
	(N=60)	*(N=22)*	*(N=21)*	*(N=17)*	
AGE (YEARS)	45 (40-47)	42 (37-47)	45 (38-51)	46 (37-51)	*0.687*
SEX (FEMALE)	18 (30%)	7 (32%)	6 (29%)	5 (29%)	*NS*
DM	2 (3.3%)	1 (4.5%)	1 (4.7%)	1 (5.9%)	*NS*
CVD	5 (8.3%)	0 (0%)	3 (14%)	2 (12%)	*NS*
CREATININE (µMOL/L)	789 (754-889)	751 (660-836)	829 (772-1077)	793 (689-892)	*0.296*
HSCRP (G/L)	1.0 (1.1-4.5)	1.0 (0.9-3.5)	0.7 (0.6-1.2)	2.2 (0.03-11.7)	***0.013***
ALBUMIN (G/L)	36 (35-37)	37 (34-38)	35 (34-37)	38 (35-39)	*0.158*
CALCIUM (µMOL/L)	2.3 (2.2-2.3)	2.2 (2.1-2.3)	2.3 (2.2-2.4)	2.3 (2.2-2.4)	*0.186*
PHOSPHATE (µMOL/L)	1.8 (1.6-1.9)	1.9 (1.6-2.0)	1.7 (1.5-2.0)	1.8 (1.4-1.9)	*0.476*
BMI (KG/M2)	23.7 (23.2-25.0)	22.8 (22.3-24.8)	24.3 (22.8-25.6)	23.6 (22.3-27.1)	*0.809*
MAP (MMHG)	105 (96-108)	109 (103-113)	102 (87-111)	103 (82-114)	*0.272*
% MEDIA CALCIFICATION	1.8 (2.2-6.8)	1.6 (1.2-7.3)	2.4 (0 -11.4)	1.5 (0-7.3)	*0.669*
CMKLR1 MRNA	1.5 (1.5- 1.9)	1.7 (1.3-2.1)	1.8 (1.3-2.2)	1.2 (1.2-2.1)	*0.808*
COL1A1 MRNA	2.4 (2.2-2.9)	2.4 (1.9-2.8)	2.3 (1.9-3.2)	2.1 (1.9-3.8)	*0.941*

Table 1: Patients characteristics and stratification into treatment groups. Continuous data presented as median (95% CI). Comparisons between groups with ANOVA on ranks.

VARIATE	ESTIMATE	STD ERROR	T RATIO	*P*
INTERCEPT	-1,644436	0,897982	-1,83	0,0837
COL1A1	0,2708344	0,114202	2,37	**0,0291**
ELASTIN	0,013812	0,024365	0,57	0,5778
ACTA2	0,078929	0,217892	0,36	0,7214
SP7	0,0389962	0,085508	0,46	0,6538
BMP2	0,0333473	0,026243	1,27	0,2200
BMP4	0,2597146	0,237762	1,09	0,2891
ENPP1	0,1275762	0,407219	0,31	0,7577
OSTEOCALCIN	0,1434931	0,139459	1,03	0,3171
AGE	0,024885	0,012379	2,01	0,0596
SEX [F]	-0,092807	0,146701	-0,63	0,5349
DIABETES [0]	0,1062533	0,196923	0,54	0,5961

Table 2: Multivariate analysis for the association of ChemR23 mRNA levels with a panel of smooth muscle cell mRNA, adjusted for age, sex and diabetes.

Figure 1

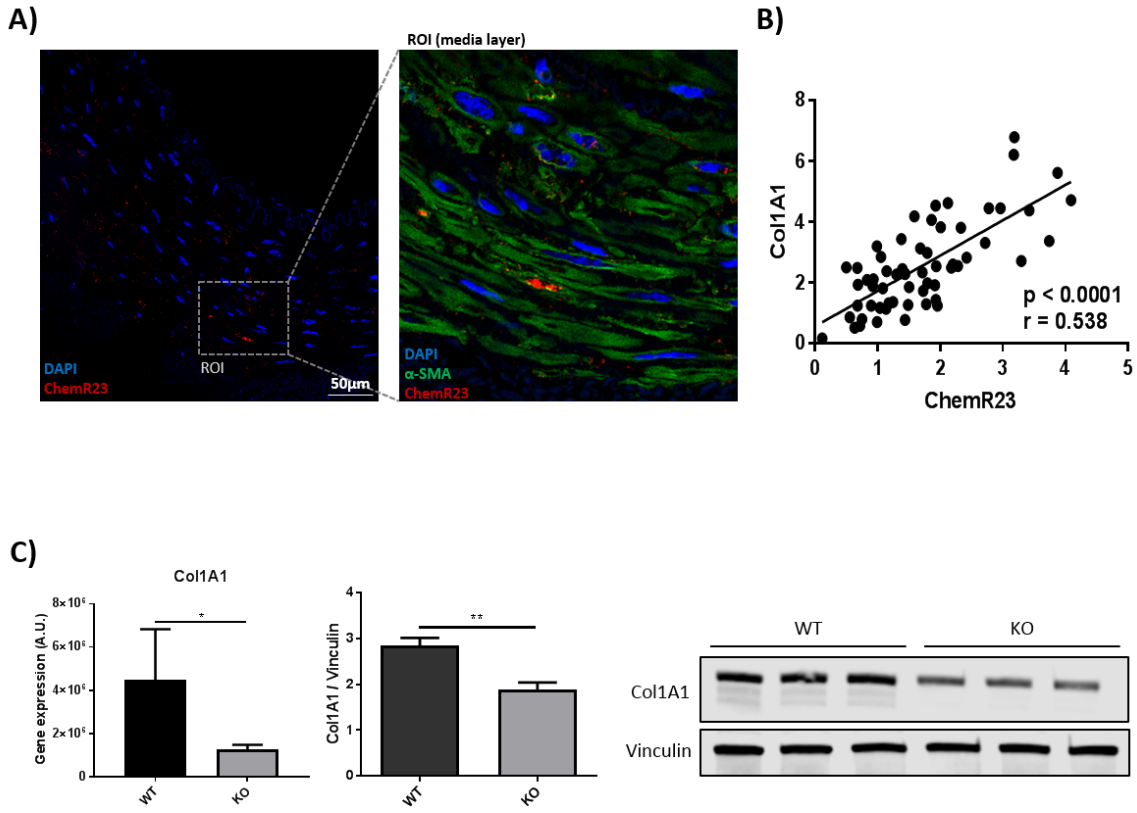

Figure 1: Collagen is related with ChemR23 expression in human and murine smooth muscle cells **(A)** Representative immunofluorescence staining of ChemR23 in the media layer of human epigastric arteries (n=4). Higher magnification image of smooth muscle cells expressing ChemR23. **(B)** Positive association between ChemR23 and Col1A1 mRNA in human arteries (n=60 patients; regression coefficient r=0.538, p<0.0001). **(C)** Mouse VSMC Col1A1 mRNA and protein expression after 24h in culture. Data represented as media ± S.D. of 3 to 5 independent experiments. * = p<0.05; ** = p<0.01.

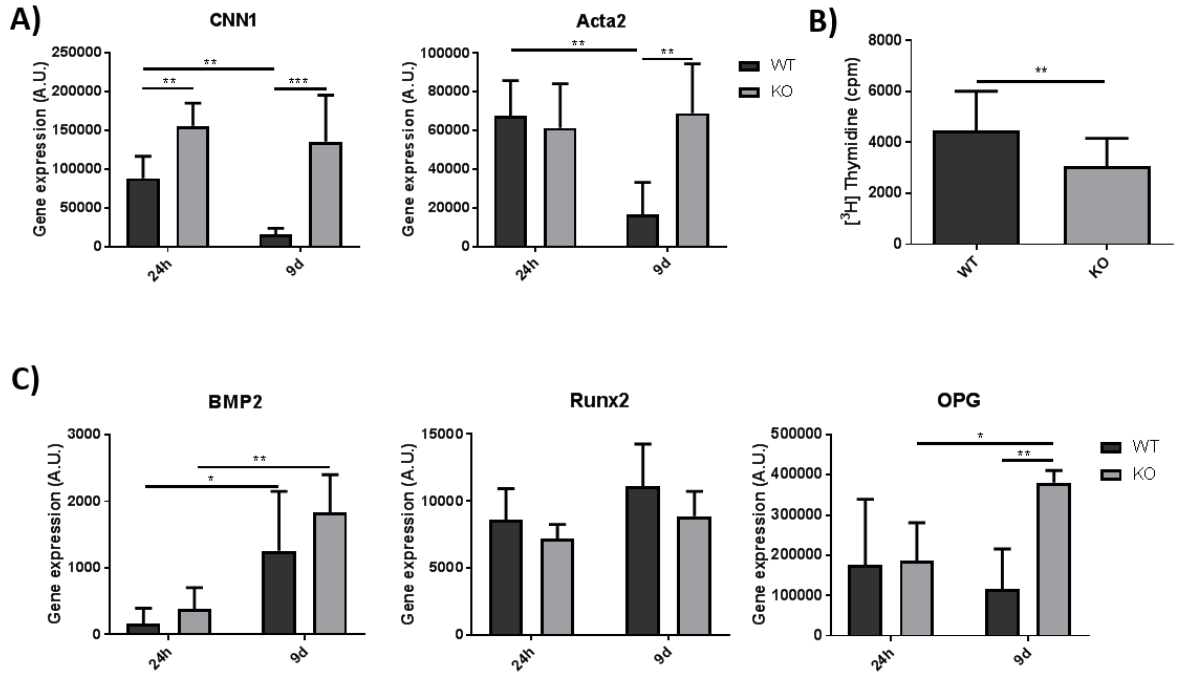

Figure 2: ChemR23 deletion alters aortic smooth muscle cell phenotype *in vitro*. (A) mRNA expression of contractile genes after 24h and 9 days in culture. **(B)** Aortic smooth muscle cell proliferation after 72h measured by ^{3}H-thymidine incorporation (expressed in counts per minute). **(C)** mRNA expression of genes relevant for calcification. Data represented as media ± S.D. of 3 to 8 independent experiments. * = $p<0.05$; ** = $p<0.01$

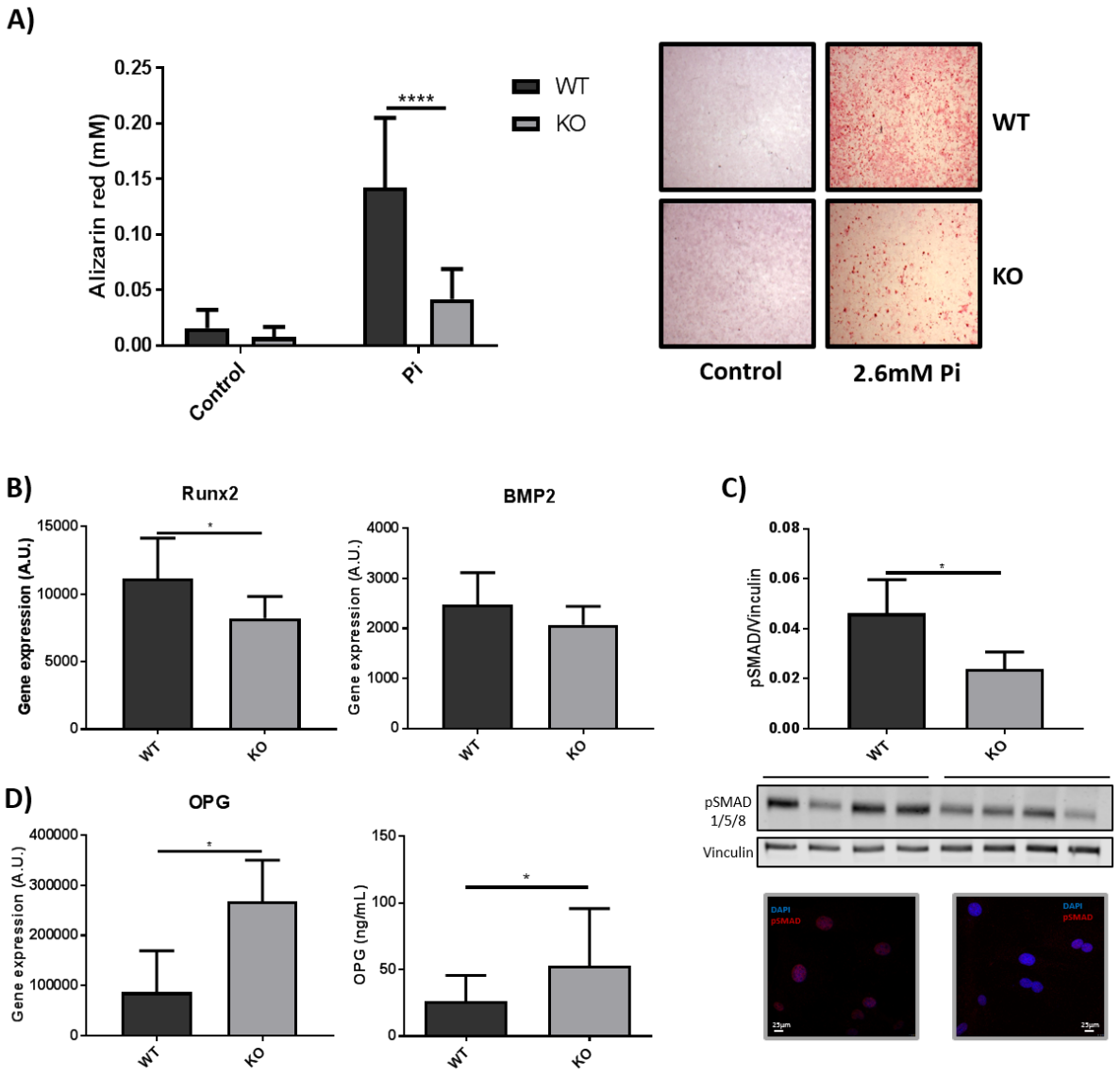

Figure 3: ChemR23 deficient VSMCs exhibit reduced calcification and osteogenic signaling. (A) Quantification of phosphate induced calcification after 9 days and representative images of alizarin red stained mouse aortic smooth muscle cells. **(B)** mRNA expression of genes involved in calcification promotion in VSMCs after 9 days in culture under calcifying conditions. **(C)** Immunoblotting and immunofluorescence against phosphorylated SMAD 1/5/8 after 30 minute stimulation with BMP-2 **(D)** mRNA expression and supernatant secreted osteoprotegerin levels. Data represented as media ± S.D. of 3 to 9 independent experiments. * = $p<0.05$; ** = $p<0.01$

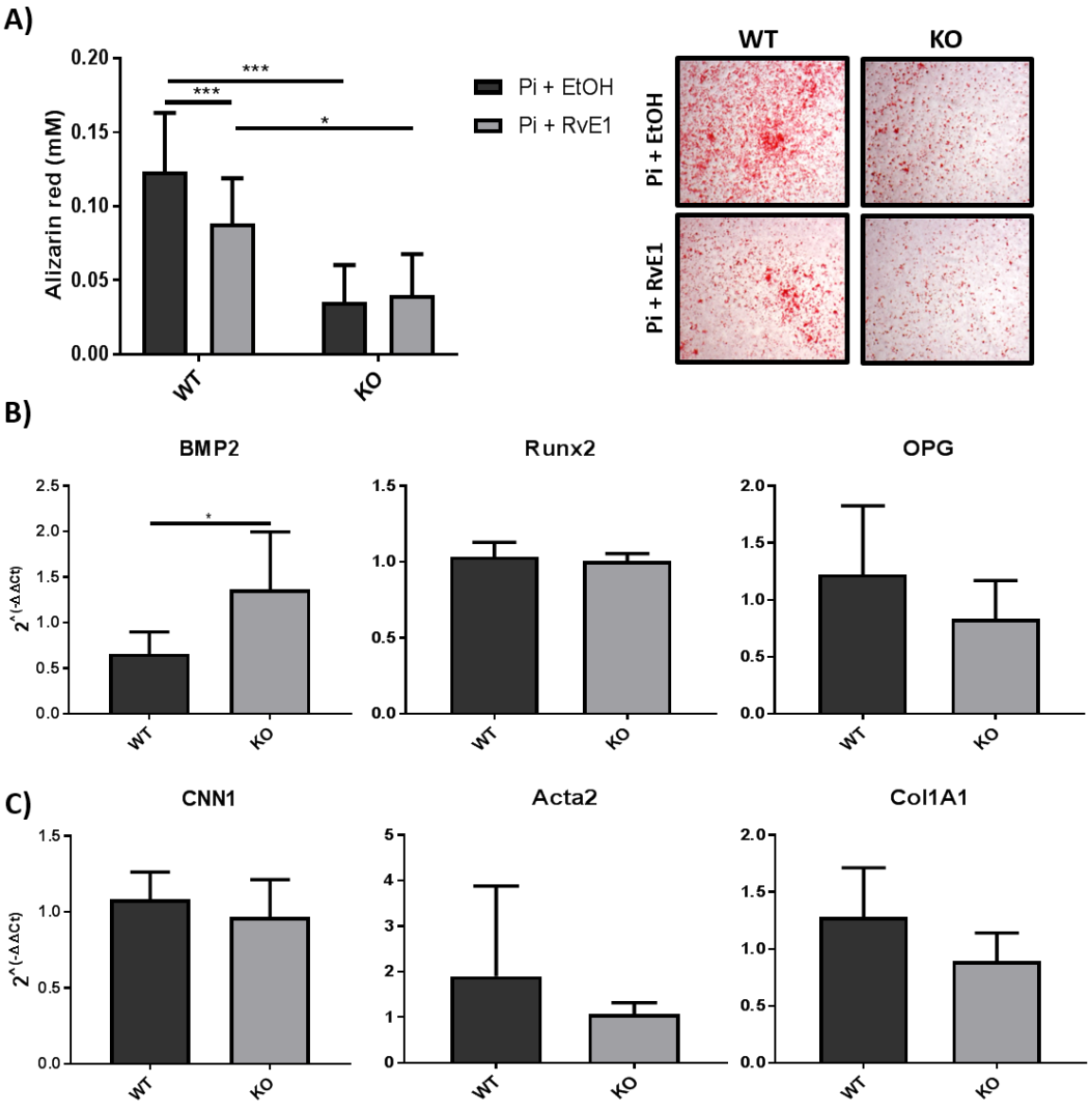

Figure 4: The ChemR23 ligand RvE1 decreases calcification and osteogenic signaling without altering VSMC phenotype. (A) Quantification of phosphate induced calcification after 9 days and representative images of alizarin red stained cells treated with vehicle (Ethanol) or RvE1. **(B)** Effect of RvE1 compared to vehicle control, after 9 days in calcifying media, in the mRNA expression of genes related with calcification **(C)** and smooth muscle cell phenotype. Data represented as media ± S.D. of 3 to 9 independent experiments. * = $p<0.05$; ** = $p<0.01$

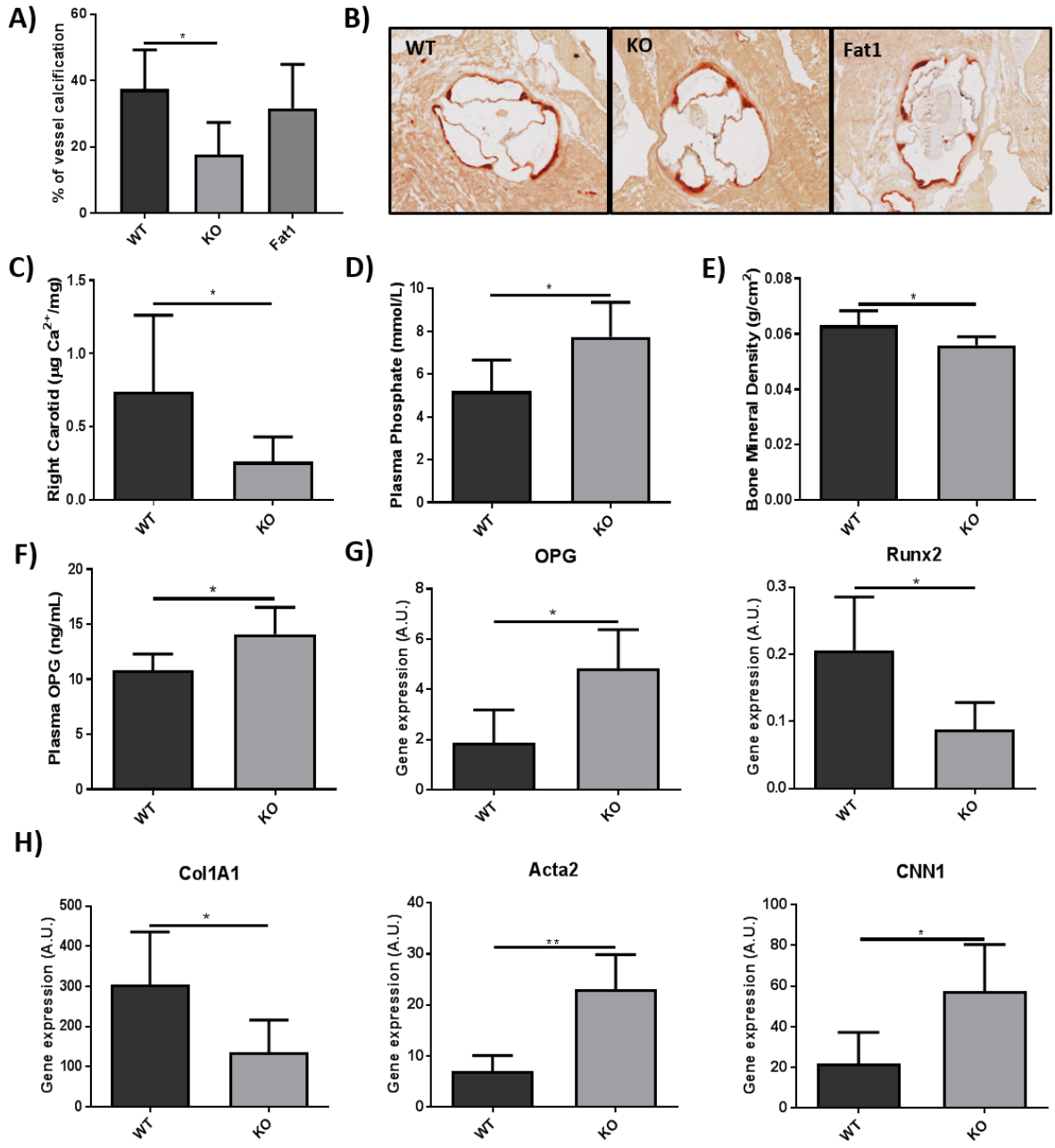

Figure 5: ChemR23 deletion, but not Fat1 transgene, protects from VitD3 induced vascular calcification in vivo. (A-B) Quantification of aortic root calcification as a percentage of the alizarin red positive area within the total vessel area, and representative images of alizarin red stained aortic roots. **(C)** Total Ca^{+2} content in the right carotid artery. **(D)** Plasma phosphate levels. **(E)** Bone mineral density of the right femur. **(F)** Plasma osteoprotegerin levels. **(G)** Aortic mRNA expression of genes involved in calcification promotion and inhibition. **(H)** Aortic mRNA expression of smooth muscle cell markers. WT n=5, KO n=7, Fat1 n=4. * = $p<0.05$; ** = $p<0.01$

Gene ID	Sequence
ChemR23	TACAGCTTGGTGTGCTTCCTCGGTC
ChemR23	TGATCTTGCACATGGCCTTCCCGAA
ChemR23	GGGTGGGATTAGATAAATGCCTGCTCT
Fat-1	CTGCACCACGCCTTCACCAACC
Fat-1	ACACAGCAGCAGATTCCAGAGATT

Supplementary table 1: Genotyping primers used in experiments.

Gene	Assay ID
CNN1	Mm00487032_m1
Acta2	Mm00725412_s1
Col1A1	Mm00801666_g1
BMP2	Mm01340178_m1
Runx2	Mm00501584_m1
OPG	Mm00435454_m1
COL1A1	Hs00164004_m1
ELN	Hs00355783_m1
ACTA2	Hs00426835_g1
SP7	Hs01866874_s1
BMP2	Hs00154192_m1
BMP4	Hs00370078_m1
ENPP1	Hs01054040_m1
BGLAP	Hs01587814_g1

Supplementary table 2: TaqMan assays used in the experiments.